

This article is licensed under a Creative Commons Attribution-NonCommercial NoDerivatives 4.0 International License.

## Epithelial–Mesenchymal Transition Contributes to Docetaxel Resistance in Human Non-Small Cell Lung Cancer

Weiwei Shen,<sup>1</sup> Hailin Pang,<sup>1</sup> Jiayu Liu, Jing Zhou, Feng Zhang, Lele Liu, Ningqiang Ma, Ning Zhang, Helong Zhang, and Lili Liu

Department of Oncology, Tangdu Hospital, the Fourth Military Medical University, Xi'an, Shaanxi, China

Lung cancer is an aggressive malignancy with high morbidity and mortality. Chemotherapy has always been the principal treatment measure, but its acquired resistance becomes a critical problem. In the current study, we established a new docetaxel-resistant human non-small lung cancer (NSCLC) cell line A549/Docetaxel. The resistance index (RI) of A549/Docetaxel cells and A549 induced by TGF- $\beta$  to docetaxel were 8.91 and 11.5, respectively. Compared to the parental A549 cells, the multiplication time of A549/Docetaxel was prolonged, the proportion of the cell cycle in the S phase decreased while that in the G<sub>1</sub> phase increased, and apoptotic rate was much lower. The morphology of the resistant cells eventuated epithelial–mesenchymal transition (EMT), which was confirmed by the higher expression of fibronectin, vimentin (mesenchymal markers), and lower expression of E-cadherin (epithelial marker) at mRNA and proteins levels. Furthermore, the representative markers for docetaxel resistance were examined, including ABCB1 (MDR1), Bcl-2, Bax, and tubulin, to figure out the mechanisms of the resistance of A549/Docetaxel. In summary, we have established a typical docetaxel-resistant human NSCLC cell line A549/Docetaxel, and it was suggested that the multidrug resistance of A549/Docetaxel was related to EMT.

Key words: Epithelial–mesenchymal transition (EMT); Human non-small cell lung cancer; Docetaxel; Drug resistance

### INTRODUCTION

Lung cancer is an aggressive malignancy with high morbidity and mortality. As to its presence of occult and its propensity to rapidly disseminate to the lymphatic system and distant organs, two thirds of patients have been inoperable at the first diagnosis. Thus, chemotherapy has always been the principal treatment measure. Docetaxel is used as the first-line chemotherapy for NSCLC, but its acquired resistance becomes a critical problem. Several mechanisms have been proposed in docetaxel resistance, such as the increased expression of the “drug pump” P-glycoprotein and MRP (1). But they are not sufficient to exhaustively explain this resistance emergence. So it is important to establish the docetaxel-resistant cell lines to further explore the more explicit drug resistance mechanisms.

Epithelial–mesenchymal transition (EMT) is a process by which epithelial cells undergo remarkable morphological changes characterized by a transition from epithelial cobblestone phenotype to elongated fibroblastic phenotype. EMT was originally identified as a crucial differentiation and morphogenetic physiological process during embryogenesis (2). Currently, EMT is recognized as a pathological

mechanism during the progression of various diseases, including inflammation, fibrosis, and cancers. The process of EMT is commonly found in most primary and metastatic tumors. Intriguingly, recent studies have shown that EMT is associated with drug resistance (3–8). In a study investigating the expression of EMT marker vimentin in drug-resistant tumor cell lines, it has been certified that both gemcitabine-resistant PC cells (MiaPaCa-2, Panc-1, and Aspc-1 cells) and adriamycin-induced drug-resistant breast cancer cells MCF7 exhibited strong expression of mesenchymal markers, including vimentin and ZEB-1 at mRNA and proteins levels (9,10).

In this study, we successfully establish a docetaxel-resistant NSCLC cell line A549/Docetaxel with stepwise increased docetaxel concentration and short-lasting exposure; in the meantime, we confirmed its association with EMT occurrence and its related drug-resistant gene. The docetaxel-resistant A549/Docetaxel could be useful as an excellent platform for the study of docetaxel-resistant mechanism and the discovery of new strategies to increase drug sensitivity toward better treatment outcome of patients diagnosed with lung cancer.

<sup>1</sup>These authors provided equal contribution to this work.

Address correspondence to Helong Zhang, Professor, Department of Oncology, Tangdu Hospital, Fourth Military Medical University, Xi'an, Shaanxi 710038, China. Tel: +13519128910; E-mail: [cnxazhl@163.com](mailto:cnxazhl@163.com) or Lili Liu, Professor, Department of Oncology, Tangdu Hospital, Fourth Military Medical University, Xi'an, Shaanxi 710038, China. E-mail: [lily123joe@yahoo.com.cn](mailto:lily123joe@yahoo.com.cn)

## MATERIALS AND METHODS

### Materials

Docetaxel and MTT were both bought from Sigma (St. Louis, MO, USA); the RT-PCR assay kit was obtained from TaKaRa (Dalian, China); the BCA assay kit was obtained from TIANGEN Biotechnology (Beijing, China); mouse against human polyclonal antibody of fibronectin, E-cadherin, vimentin, rabbit against human polyclonal antibody of ABCB1, Bcl-2, and Bax were obtained from Abcam (Cambridge, MA, USA); mouse against human monoclonal antibody of tubulin and  $\beta$ -actin were obtained from Sigma; HRP-labeled goat against mouse/rabbit second antibody were obtained from ZHONGSHAN Biotechnology (Beijing, China); and the ECL assay kit was obtained from Thermo (Rockford, IL, USA). Transwell was purchased from BD Corning.

### Cell Culture

The human lung adenocarcinoma cell line A549 was purchased from American Type Culture Collection (ATCC, Rockville, MD, USA) and preserved in our institute. The A549 cells were maintained in RPMI-1640 with 10% fetal bovine serum (Life Technologies Corporation, Grand Island, NY, USA) and incubated at 37°C in a humidified atmosphere of 5% CO<sub>2</sub>, and 500 ng/ml docetaxel was added to A549/Docetaxel culture medium to maintain their resistant phenotype.

### Establishment of Docetaxel-Resistant A549/Docetaxel

The A549 cells of logarithmic phase were exposed for 24 h every time to stepwise increased concentration of docetaxel from 1 ng/ml to 1,000 ng/ml. During this procedure, a few surviving cells proliferated and recolonized the cultures, yielding a docetaxel-resistant strain. The subline was designated A549/Docetaxel.

### Evaluation of A549/Docetaxel Drug Resistance Level

To assess the sensitivity of the A549/Docetaxel cell line to docetaxel, a cytotoxicity assay was carried out using 3-[4,5-dimethylthiazol-2-yl]-2,5-diphenyl tetrazolium bromide (MTT). In brief, A549 and A549/Docetaxel cells were harvested, counted, and seeded into 96-well plates at  $2 \times 10^4$ /well. The cells were incubated for 24 h prior to the addition of the docetaxel, which was diluted to a range of concentrations. The cells exposed to culture medium served as a control. After incubation for 72 h, 20  $\mu$ l MTT (5 mg/ml) was added to the cells and incubated at 37°C for 3 h. The MTT solution was removed, and 150  $\mu$ l DMSO was added to each well to dissolve the blue formazan crystals. The optical density was measured at 490-nm wavelengths using Model 680 microplate reader (Bio-Rad). IC<sub>50</sub> values (the concentration of drugs that produced a 50% reduction of absorbance) of treated and untreated cells were analyzed. The resistance index

(RI) = IC<sub>50</sub>(549/Docetaxel)/IC<sub>50</sub>(A549). To gain accuracy, four wells were used for each condition, and three independent MTT assays were repeated.

### Cell Proliferation Assay

A549 and A549/Docetaxel cells were harvested, counted, and seeded into 96-well plates at  $1 \times 10^3$ /well. Every day, one 96-well plate was taken out for test from the second day, repeating 5 days. MTT was used to examine the cell proliferative rate. Assays were repeated three times for accuracy.

### Flow Cytometry Analysis

Flow cytometry analysis was used to determine the distribution of cells in cell cycle and performed as described. Briefly, cells were collected and suspended with 1 ml of 70% alcohol and kept at 4°C for 30 min, followed by being washed and resuspended with cool PBS. Then, 5  $\mu$ l RNase (10 mg/ml) was added and fixed for 1 h at 37°C; cells were stained with 100  $\mu$ g/ml propidium iodide in 0.1% sodium citrate/0.1% Triton X-100 solution for 30 min at RT in the dark. Finally, the cells were washed with cool PBS twice again. Analysis of cellular DNA content was performed by flow cytometry at an excitation wavelength of 488 nm. The distribution of cells in three major phases of the cycle (G<sub>1</sub>, S, and G<sub>2</sub>/M) was analyzed using CellQuest and MidFit software (BD).

Cell apoptosis was determined by flow cytometry. The Annexin-V-FITC-PI kit (Key GEN, Nanjing, China) was used to detect apoptosis. The cells were collected and washed with cool PBS twice and were resuspended in 200  $\mu$ l  $1 \times$  binding buffer; 10  $\mu$ l of Annexin V-FITC and 5  $\mu$ l of PI were added and incubated at room temperature for 15 min in the dark. Finally, 300  $\mu$ l of binding buffer was added into the mixture and analyzed with the FACS Calibur system (BD).

### RT-PCR Analysis

Total RNA was extracted using Trizol reagent (Invitrogen, Carlsbad, CA, USA) according to the manufacturer's instructions; 1  $\mu$ g of RNA was subjected to reverse transcription. The PCR primers used are shown in Table 1. The PCR products were separated on a 1% agarose gel and visualized and photographed under ultraviolet light.

### Western Blot Analysis

After protein quantization using the BCA kit, 50  $\mu$ g of protein was boiled in loading buffer, resolved on 10% SDS-polyacrylamide gels, electrotransferred to nitrocellulose membranes, and incubated overnight with mouse polyclonal antibodies against fibronectin (1:800), E-cadherin (1:500), and vimentin (1:800), rabbit polyclonal against Bcl-2 (1:1,000), ABCB1 (1:500), Bax (1:500), and mouse

**Table 1.** Primers Used

mRNA	Forward 5'–3'	Reverse 5'–3'
Fibronectin	ATTGGAGACACGTGGAGCAA	TCCGGCTGAAGCACTTTGTA
Vimentin	AGATGGCCCTTGACATTGAG	TGGAAGAGGCAGAGAAATCC
E-cadherin	ACAGCCCCGCCTTATGATT	TCGGAACCGCTTCCTTCA
Bcl-2	CGACTTCGCCGAGATGTCCAGCCAG	CTTGTGGCTCAGATAGGCACCCAGG
Bax	CAGCTCTGAGCAGATCATGAAGACA	GCCCATCTTCTCCAGATGGTGAGC
Tubulin	5'-CAGATGCTTAACGTGGAGAACAAGA	5'-CACGAGGTGGGATGTCCACAGA
ABCB1	GGGATGGTCAGTGTGATGGA	GCTATCGTGGTGGCAAACAATA'
$\beta$ -Actin	GATCATTGCTCCTCCTGAGC	CACCTTCACCGTTCCAGTTT

monoclonal against tubulin (1:50),  $\beta$ -actin (1:5,000). The secondary antibodies (1:5,000; anti-mouse/rabbit) were applied, and the relative content of the target proteins was detected by chemiluminescence.

#### Cell Migration and Invasion Assay

Transwell invasion assays were performed in Transwell inserts (pore size, 8  $\mu$ m thick) in a 24-well companion plate (both from BD Corning). Inserts were coated with a 70- $\mu$ l Matrigel basement membrane matrix (diluted in 1:8; BD Corning). A549 and A549/Docetaxel cells ( $2 \times 10^4$ /well) were seeded in triplicates into inserts in RPMI-1640 without FBS. Besides, 500  $\mu$ l of medium containing 10% FBS was added into the bottom chamber to serve as a chemoattractant. After 24 h of incubation, cells that migrated through the Matrigel were fixed with 95% ethyl alcohol and then stained with 0.5% crystal violet. Invading cells on the bottom of the filters were imaged by microscopy (200 $\times$ ). However, only one step was different between the migration assay and invasion assay, which was that the inserts in the migration assay were not coated with Matrigel basement membrane matrix.

#### Colony Formation Assay

Two hundred A549 and A549/Docetaxel cells were plated at equal density in a six-well plate. They were divided into three groups (A, B, and C), and every group included two wells. After 24 h of incubation, TGF- $\beta$  (10 ng/ml) was added into group B. Docetaxel was added into either one well of every group to investigate the effect of docetaxel (12.5 ng/ml) on the colony formation of A549 and A549/Docetaxel cells. Incubated for 2 weeks, the cells were stained with 0.25% crystal violet, and the number of colonies was counted manually. Triplicate plates were set up for accuracy.

#### Statistical Analysis

Statistical analysis was performed with the SPSS 13.0 software package. Values were presented as the mean  $\pm$  SEM. Statistical significance was evaluated using the Student's two-tailed *t* test;  $p < 0.05$  was considered statistically significant.

## RESULTS

#### Establishment of Docetaxel-Resistant Cell Lines

A docetaxel-resistant subline derived from the parental-sensitive cell line A549 was successfully established by stepwise selection in docetaxel over a period of 8 months, designated A549/Docetaxel. It can grow properly in the complete medium with 500 ng/ml docetaxel. The RI of A549 induced by TGF- $\beta$  and A549/Docetaxel against docetaxel was 8.91 and 11.50, respectively (Table 2).

#### Cell Proliferation of A549/Docetaxel

Next, we performed experiments to determine A549/Docetaxel proliferation characteristics. The growth curve demonstrated that the A549/Docetaxel proliferated slowly with the delay of the split peak and prolonged doubling time in comparison with the A549 (Fig. 1), which was actually consistent with the proliferation features of the drug-resistant cell lines.

#### Cell Cycle Analysis of A549/Docetaxel

We performed experiments to test whether the changes in cell cycle contributed to the resistance capability of the A549/Docetaxel. As shown in Figure 2A and C, the percentage of G<sub>1</sub> phase in the A549/Docetaxel group ( $50.5 \pm 2.8$ ) was much higher than that in the A549 group ( $41.5 \pm 2.3$ ) ( $p < 0.05$ ), while the percentage of S phase ( $37.3 \pm 1.6$ ) was lower than the A549 group ( $49.2 \pm 2.5$ ) ( $p < 0.05$ ). However, after the treatment of docetaxel (500 ng/ml) for 24 h, the A549/Docetaxel group has a relatively higher proportion in the S phase

**Table 2.** IC Values (ng/ml) of Docetaxel for A549, A549 Induced by TGF- $\beta$ , and A549/Docetaxel

Group	IC <sub>50</sub>	RI	P
A549	22,387.2 $\pm$ 0.6		
A549+TGF- $\beta$	144,727.0 $\pm$ 1.3	11.50	<0.01
A549/Docetaxel	112,201.8 $\pm$ 1.2	8.91	<0.01

Survival rates of NSCLC cells to anticancer drugs were evaluated by MTT assay. Data were represented as mean  $\pm$  SD of three independent experiments.

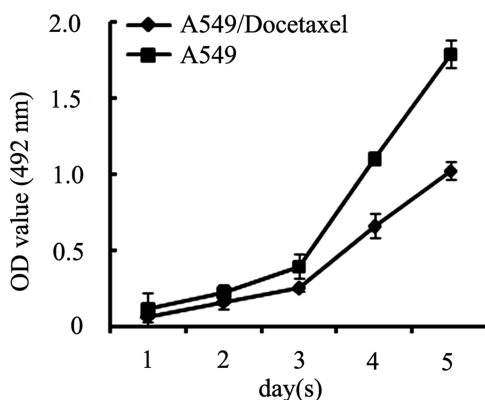


**Figure 1.** Cell proliferation assay. Growth curve determined by MTT assay to represent slow proliferate rate of A549/Docetaxel cells with delayed split peak and prolonged multiplication time compared with A549 cells.

( $25.9 \pm 3.1/4.2 \pm 2.1$ ) and  $G_1$  phase ( $45.2 \pm 2.6/4.1 \pm 3.5$ ) and a much lower proportion in the  $G_2/M$  phase ( $28.9 \pm 2.4/91.7 \pm 3.5$ ) compared with the A549 group ( $p < 0.01$ ) (Fig. 2B and D). These results suggested that the changes of cell cycle distribution in the A549/Docetaxel cells contributed to slow down cell proliferation via induction of  $G_1$  phase arrest and inhibition of the S phase entry, and docetaxel can induce  $G_2/M$  phase arrest in the A549 cells, while the A549/Docetaxel cells can reverse this phenomenon, which may partly contribute to its resistance characteristics.

#### Cell Apoptosis of A549/Docetaxel

Because the blockage of apoptosis is an important factor of the drug resistance of cancer cells, we used flow cytometry to detect the apoptosis capacity of A549 and

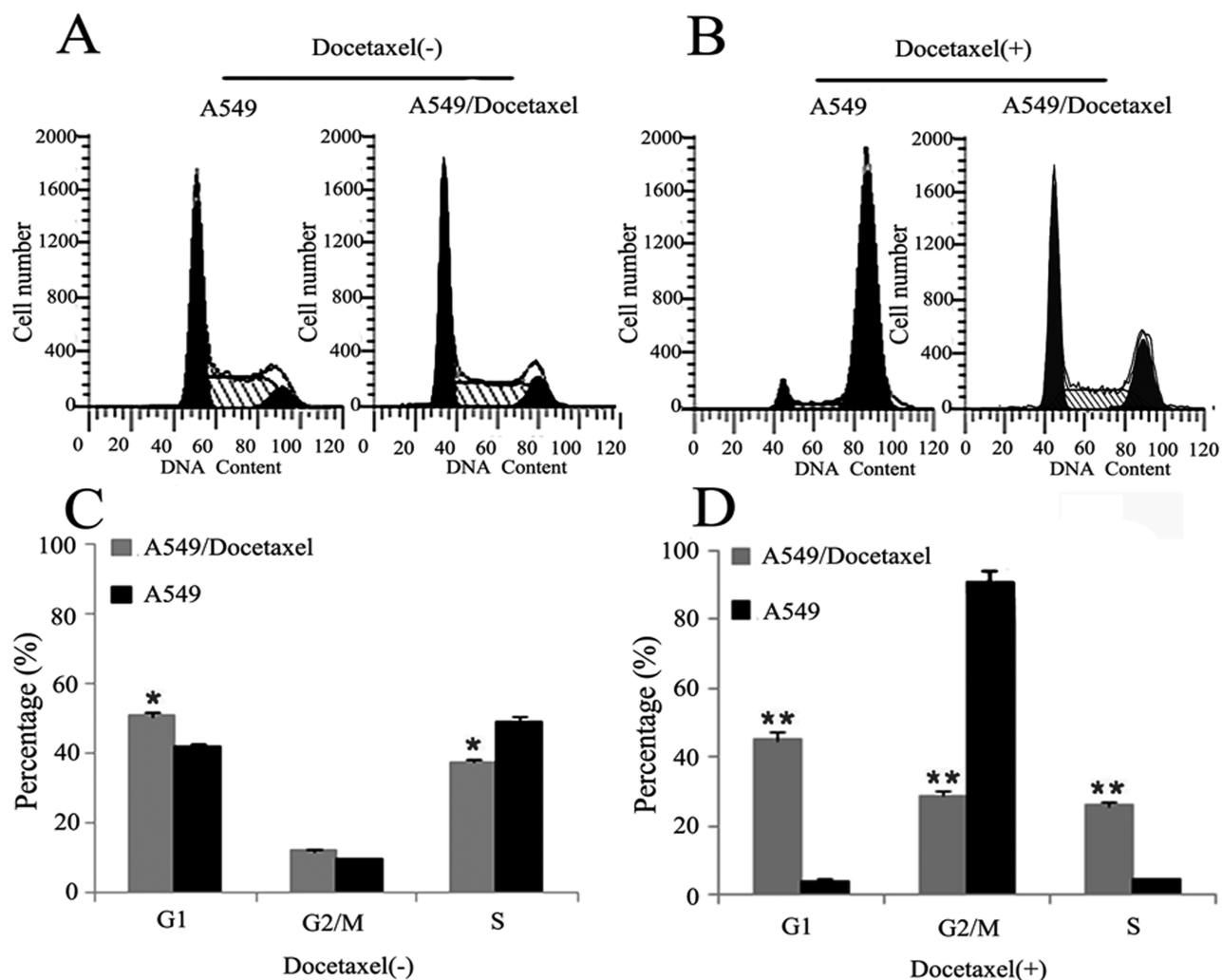


**Figure 2.** Cell cycle analysis was determined by flow cytometry. Cell cycle analysis of A549/Docetaxel and A549 cells without (A, C) and with (B, D) the treatment of docetaxel (500 ng/ml) (\* $p < 0.05$ , \*\* $p < 0.01$ ).



A549/Docetaxel cells in the presence of docetaxel. The apoptosis rates of A549/Docetaxel and A549 cells were  $0.5 \pm 0.2\%$  and  $1.9 \pm 0.5\%$  respectively,  $3.2 \pm 0.4\%$  and  $64.1 \pm 0.6\%$  with docetaxel (500 ng/ml) treatment for 24 h ( $p < 0.01$ ). The apoptosis rate of A549/Docetaxel

was 1/23.1 of A549 cells after the effect of docetaxel treatment, while without the docetaxel, the apoptosis rate of A549/Docetaxel was 1/3.8 of A549 (Fig. 3). This assay indicated that docetaxel resistance of A549/Docetaxel cells may associate with the apoptotic potential.

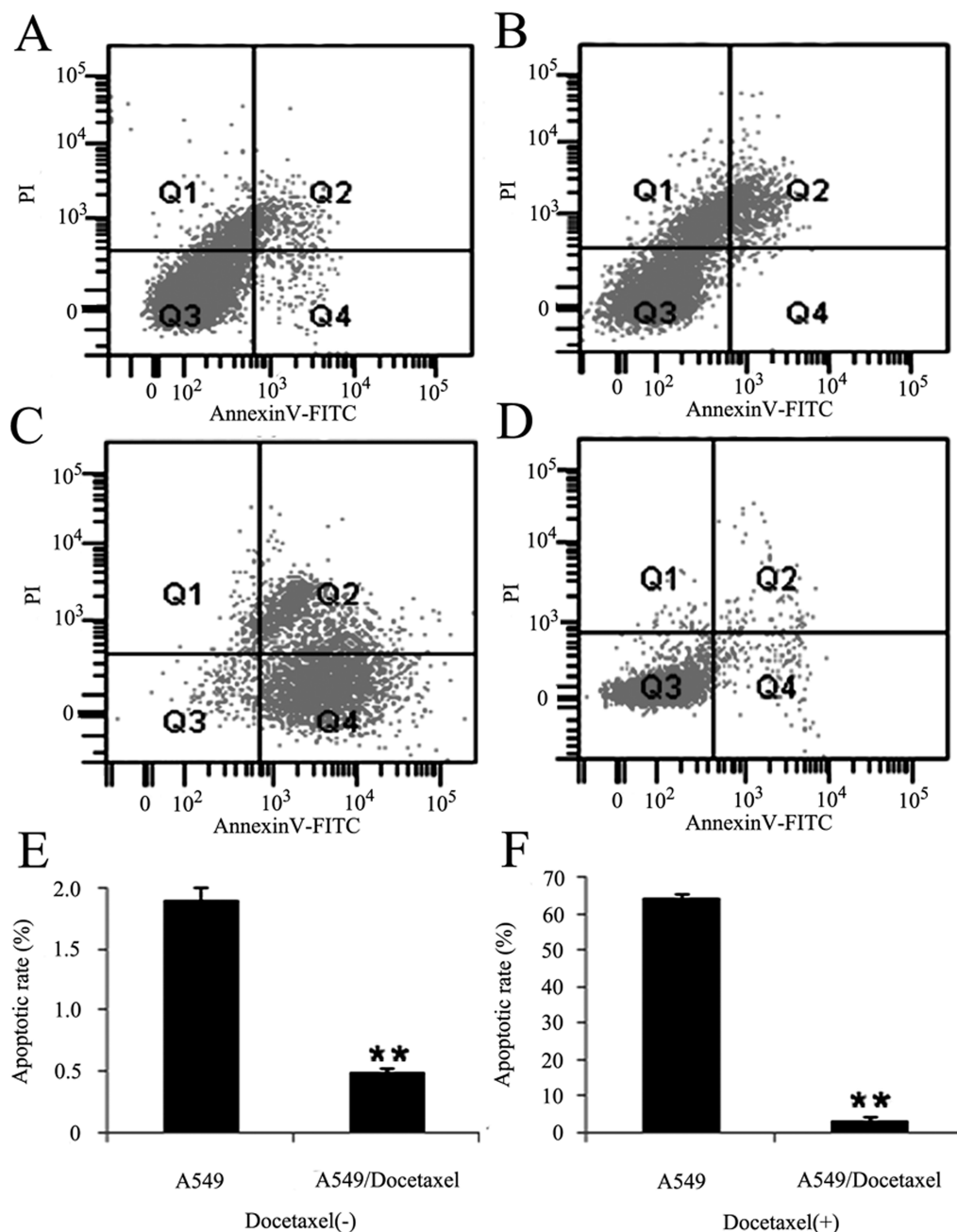


**Figure 3.** Cell apoptosis was performed by the Annexin-V-FITC-PI kit. A549 and A549/Docetaxel cells were stained with Annexin-V-FITC and PI, detected by FACS Calibur. Annexin-V-FITC (-)/PI (-) indicates survival cells, while Annexin-V-FITC (+)/PI (+) indicates cells in the stage of necrosis, and Annexin-V-FITC (+)/PI (-) indicates cells in the stage of apoptosis. The representative image of (A) A549 cells and (B) A549/Docetaxel cells, (C) A549 cells, and (D) A549/Docetaxel cells with the effect of docetaxel (500 ng/ml) for 24 h. The percentage of apoptotic A549 and A549/Docetaxel cells incubated in (E) common medium or in (F) 500 ng/ml docetaxel for 24 h. These values were given as mean  $\pm$  SD (\*\* $p < 0.01$ ).

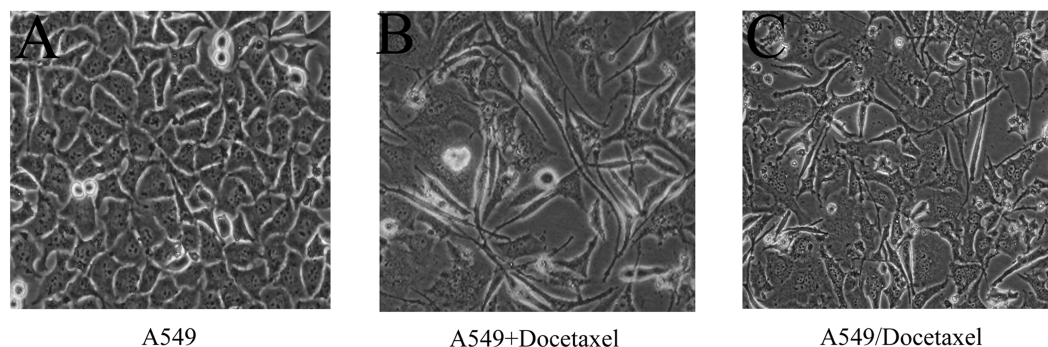


**Figure 4.** The morphological changes during the establishment of A549/Docetaxel (200 $\times$ ) examined by light microscope. (A) The original morphology of A549. (B) The morphology of A549 with the treatment of docetaxel at the beginning. (C) The morphology of the A549/Docetaxel with a more obvious “mesenchymal” phenotype.

#### *Cellular Morphology and the Expression of EMT Markers*

Simple light microscopic analysis of the cell phenotype confirmed that the A549 cells were uniform in shape and grew in tightly adherent “sheets” of cells in monolayer culture. However, the A549/Docetaxel cells were irregular in shape and did not form close attachments in culture, indicating that the A549/Docetaxel displayed a more “mesenchymal” phenotype (Fig. 4).

To further confirm our observation, we assessed the levels of E-cadherin (epithelial marker), fibronectin, and vimentin (mesenchymal marker) by RT-PCR and Western blot. A statistically significant increased expression of fibronectin and vimentin accompanied with reduced expression of E-cadherin were observed in A549/Docetaxel cells, which was actually consistent with the EMT phenotype (Fig. 5). These results proved that the docetaxel resistance of A549/Docetaxel might be related to EMT.

#### *Increased Migratory and Invasive Potential of A549/Docetaxel*

The EMT program is associated with enhanced cancer invasiveness. Therefore, we next compared migratory ability and invasive potential between the A549 and

A549/Docetaxel cells. As shown in Figure 6, more A549/Docetaxel cells migrated through the insert. However, a more significant difference was shown in the invasive assay, in which a distinct number of A549/Docetaxel invaded through the Matrigel. In a word, A549/Docetaxel acquired an increased malignant behavior contrasted with the A549 cell.

#### *The Ability of A549/Docetaxel to Form Colonies*

In order to detect the ability to form colonies of A549/Docetaxel, the colony formation assay was performed. The colonies formed by A549/Docetaxel cells were smaller than their parental cells in a condition without docetaxel. Besides, we observed that TGF- $\beta$  could promote A549 cells to form colonies. However, when docetaxel was present in the medium, A549/Docetaxel cells and A549 cells induced by TGF- $\beta$  were still able to form colonies, while the parental cells lost this potential (Fig. 7).

#### *The Mechanism of the Resistance of A549/Docetaxel*

The representative markers for drug resistance, including ABCB1, Bcl-2, Bax, and tubulin were examined from mRNA (data not shown) and protein (Fig. 8) levels. The results indicated that ABCB1, Bcl-2, and tubulin were

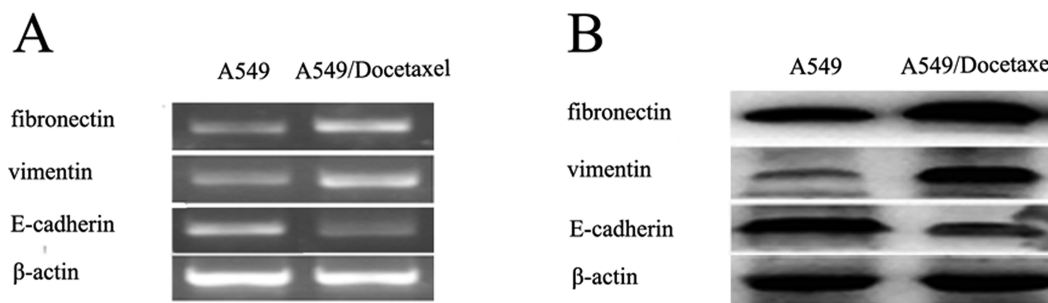


**Figure 5.** Differentially expressed EMT molecules between A549/Docetaxel and A549 determined by RT-PCR (A) and Western blot (B).  $\beta$ -Actin was used as an internal control.

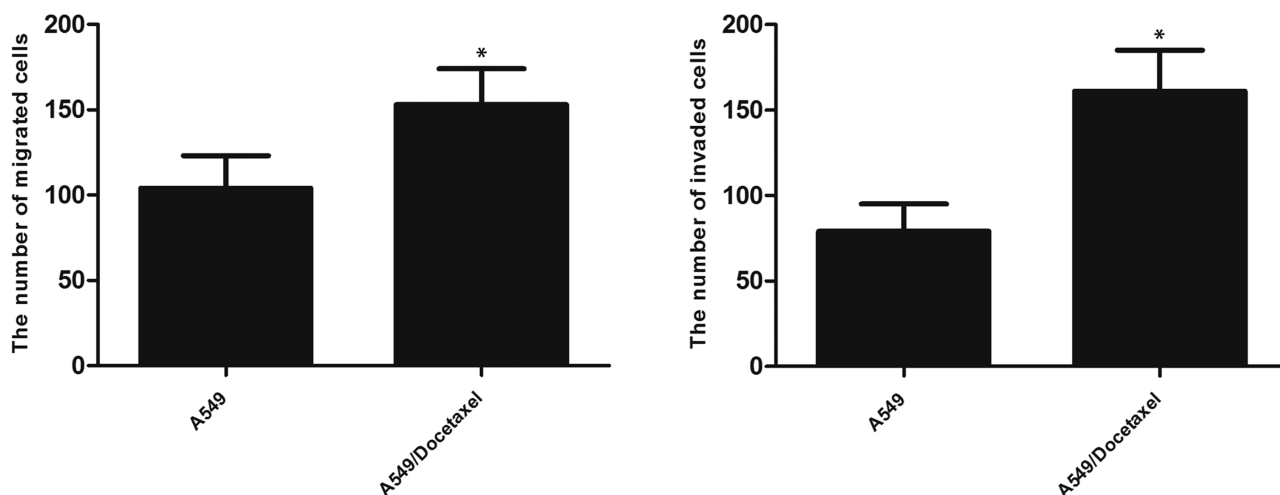


**Figure 6.** Quantitative analysis of the cells migrating and invading through the Transwell chambers (\* $p < 0.05$ ).

upregulated, while Bax was downregulated in A549/Docetaxel compared to A549.

### DISCUSSION

Resistance to chemotherapeutic agents is becoming a major impediment for the treatment of patients with NSCLC. It was generally considered that cell phenotype was associated with the drug resistance, suggesting that mesenchymal-type tumor cells were more resistant to chemotherapeutics than epithelial-type tumor cells (6,11). EMT has been shown to be an important step in inducing drug resistance of cancer

cells against conventional therapeutics (6,12–14). Many researchers have demonstrated that alterations in the expression of critical molecules have been observed during the acquisition of EMT phenotype (15–17), consistent with their association in cellular signal transduction pathways. In our study, it was confirmed that TGF- $\beta$ , a well-known inducer of EMT, not only can promote parental A549 cells to transform into mesenchymal type and to form colonies but also can sustain this ability in the presence of docetaxel, further indicating that EMT played an important role in changing the biological behaviors of A549 cells.

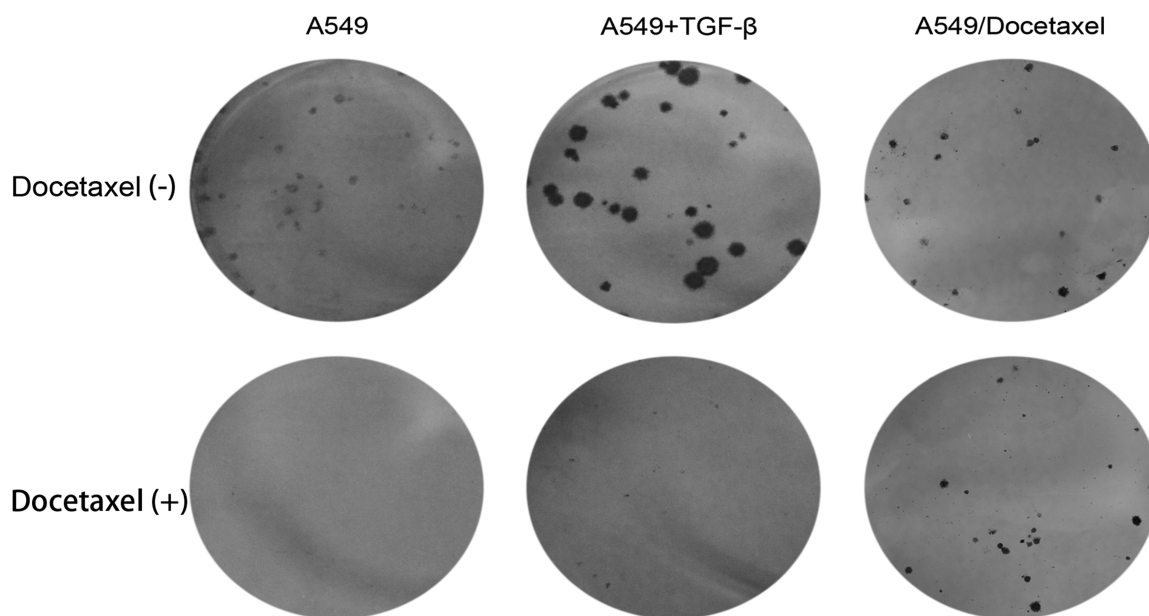


**Figure 7.** The colonies formed by A549, A549 induced by TGF- $\beta$ , and A549/Docetaxel. A549 and A549/Docetaxel cells were plated at equal density in six-well plates and incubated with or without docetaxel for 2 weeks. Representative images of colonies formed by A549, A549 induced by TGF- $\beta$ , and A549/Docetaxel with or without docetaxel are shown.

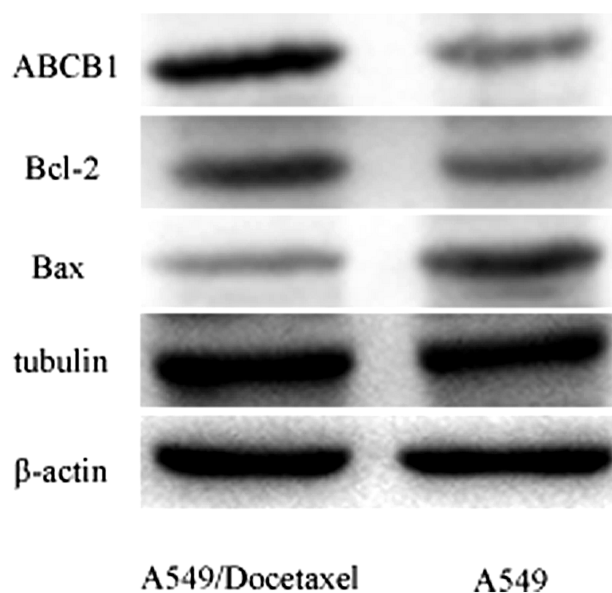


**Figure 8.** The expression of ABCB1 (MDR1), Bcl-2, Bax, and tubulin in A549 and A549/Docetaxel at protein level. The expression at mRNA level was not shown.

Jin Ren et al. had established a docetaxel-resistant human lung adenocarcinoma cell line (SPC-A1/DTX), which showed a typical mesenchymal phenotype, accompanied by increased migratory and invasive capacity both in vitro and in vivo (18). Consistently, in this study, A549/Docetaxel, a cell line against docetaxel originated from A549 cells, exhibited EMT characteristics and enhanced migratory and invasive potential. However, the mechanisms of chemoresistance are not very clear.

The cell apoptosis results showed the blockage of apoptotic A549/Docetaxel cells contributed greatly to its docetaxel resistance, which was consistent with the MDR (multidrug resistance) mechanisms. Defects in cell death signaling are a hallmark of cancer, particularly apoptotic cell death, which is often inhibited in tumor cells due to overexpression of antiapoptotic proteins or decreased expression of proapoptotic proteins. For example, the Bcl-2 gene has been shown to be overexpressed in many solid tumor cell lines, contributing to resistance to chemotherapy and radiotherapy (19). Furthermore, it has been demonstrated that downregulation of Bcl-2 sensitizes cells to chemotherapy, whereas a loss of Bax expression results in increased resistance (20). Besides, ABCB1 and tubulin have also been reported to contribute to MDR. ABCB1 is one of the ATP-binding cassette (ABC) family and can enhance the function of the drug-efflux pump, which eventually leads to reduced intracellular concentration of drugs in multidrug resistance cancer cells. It has been found to be upregulated in A549/D16 cells, associating with drug resistance and drug

transport (21). As the fundamental unit of microtubules, tubulin is critically involved in chromosomal segregation, cell division, motility, and intracellular transportation and has been considered as a potential anticancer drug target (22). In this study, we confirmed that ABCB1, Bcl-2, Bax, and tubulin contribute to the chemoresistance of A549/Docetaxel.

Multidrug resistance in tumors is common, and clinical unresponsiveness to antineoplastics correlates with in vitro chemotherapy resistance for some solid tumors (23–25). Recently, the prevalence of chemoresistance in resected NSCLC tumor cultures to several individual antineoplastic drugs was reported (26). The clinical utility of in vitro chemotherapy resistance assays to estimate clinical response to chemotherapy has been debated for nearly a decade. Kern and Weisenthal (27) compared clinical response to chemotherapy with an independent tumor set of 450 human tumor cell cultures, 20 of which were NSCLC; the ability of the extreme drug resistance assay to predict tumor resistance to an agent was over 99% specific. Accordingly, this phenomenon has been examined in breast cancer and resulted in that the median time to survival and disease progression was distinctly shorter for patients treated with any combination of agents exhibiting either extreme or intermediate in vitro drug resistance in comparison with patients having tumors with low in vitro resistance to both drugs (23). In vitro drug resistance is associated with a shorter survival similar to that correlated with advanced stage or positive lymph node metastasis. Further studies on the relationship between in vitro chemotherapy resistance testing as it relates to clinical response or prognosis are ongoing. Therefore, the application of tumor chemotherapy resistance testing may be of clinical benefit.

In summary, we have established a typical docetaxel-resistant human NSCLC cell line A549/Docetaxel, and it was suggested that the multidrug resistance of A549/Docetaxel was related to EMT. ABCB1 (MDR1), Bcl-2, Bax, and tubulin may contribute the chemoresistance of A549/Docetaxel. The A549/Docetaxel cells could be useful as an excellent platform for the study of docetaxel-resistant mechanisms and the discovery of new strategies to increase drug sensitivity toward better treatment outcome of patients diagnosed with lung cancer.

**ACKNOWLEDGMENTS:** This work was supported by the National Nature Science Foundation of China (Number: 81272348, 81301990). The authors declare no conflicts of interest.

## REFERENCES

1. Wilson, T. R.; Longley, D. B.; Johnston, P. G. Chemoresistance in solid tumours. *Ann. Oncol.* 17(Suppl. 10): x315–24; 2006.
2. Thiery, J. P.; Sleeman, J. P. Complex networks orchestrate epithelial-mesenchymal transitions. *Nat. Rev. Mol. Cell Biol.* 7:131–42; 2006.



3. DiMeo, T. A.; Anderson, K.; Phadke, P.; Fan, C.; Perou, C. M.; Naber, S.; Kuperwasser, C. A novel lung metastasis signature links Wnt signaling with cancer cell self-renewal and epithelial-mesenchymal transition in basal-like breast cancer. *Cancer Res.* 69:5364–73; 2009.
4. Kudo-Saito, C.; Shirako, H.; Takeuchi, T.; Kawakami, Y. Cancer metastasis is accelerated through immunosuppression during Snail-induced EMT of cancer cells. *Cancer Cell* 15:195–206; 2009.
5. Tsuji, T.; Ibaragi, S.; Hu, G. F. Epithelial-mesenchymal transition and cell cooperativity in metastasis. *Cancer Res.* 69:7135–9; 2009.
6. Fuchs, B. C.; Fujii, T.; Dorfman, J. D.; Goodwin, J. M.; Zhu, A. X.; Lanuti, M.; Tanabe, K. K. Epithelial-to-mesenchymal transition and integrin-linked kinase mediate sensitivity to epidermal growth factor receptor inhibition in human hepatoma cells. *Cancer Res.* 68:2391–9; 2008.
7. Christiansen, J. J.; Rajasekaran, A. K. Reassessing epithelial to mesenchymal transition as a prerequisite for carcinoma invasion and metastasis. *Cancer Res.* 66:8319–26; 2006.
8. Cheng, G. Z.; Chan, J.; Wang, Q.; Zhang, W.; Sun, C. D.; Wang, L. H. Twist transcriptionally up-regulates AKT2 in breast cancer cells leading to increased migration, invasion, and resistance to paclitaxel. *Cancer Res.* 67:1979–87; 2007.
9. Li, Q. Q.; Xu, J. D.; Wang, W. J.; Cao, X. X.; Chen, Q.; Tang, F.; Chen, Z. Q.; Liu, X. P.; Xu, Z. D. Twist1-mediated adriamycin-induced epithelial-mesenchymal transition relates to multidrug resistance and invasive potential in breast cancer cells. *Clin. Cancer Res.* 15:2657–65; 2009.
10. Li, Y.; VandenBoom, T. N.; Kong, D.; Wang, Z.; Ali, S.; Philip, P. A.; Sarkar, F. H. Up-regulation of miR-200 and let-7 by natural agents leads to the reversal of epithelial-to-mesenchymal transition in gemcitabine-resistant pancreatic cancer cells. *Cancer Res.* 69:6704–12; 2009.
11. Maseki, S.; Ijichi, K.; Tanaka, H.; Fujii, M.; Hasegawa, Y.; Ogawa, T.; Murakami, S.; Kondo, E.; Nakanishi, H. Acquisition of EMT phenotype in the gefitinib-resistant cells of a head and neck squamous cell carcinoma cell line through Akt/GSK-3beta/snail signalling pathway. *Br. J. Cancer* 106:1196–204; 2012.
12. Chang, T. H.; Tsai, M. F.; Su, K. Y.; Wu, S. G.; Huang, C. P.; Yu, S. L.; Yu, Y. L.; Lan, C. C.; Yang, C. H.; Lin, S. B.; Wu, C. P.; Shih, J. Y.; Yang, P. C. Slug confers resistance to the epidermal growth factor receptor tyrosine kinase inhibitor. *Am. J. Respir. Crit. Care Med.* 183:1071–9; 2011.
13. McConkey, D. J.; Choi, W.; Marquis, L.; Martin, F.; Williams, M. B.; Shah, J.; Svatek, R.; Das, A.; Adam, L.; Kamat, A.; Siefker-Radtke, A.; Dinney, C. Role of epithelial-to-mesenchymal transition (EMT) in drug sensitivity and metastasis in bladder cancer. *Cancer Metastasis Rev.* 28:335–44; 2009.
14. Sabbah, M.; Emami, S.; Redeuilh, G.; Julien, S.; Prevost, G.; Zimmer, A.; Ouelaa, R.; Bracke, M.; De Wever, O.; Gespach, C. Molecular signature and therapeutic perspective of the epithelial-to-mesenchymal transitions in epithelial cancers. *Drug Resist. Updates* 11:123–51; 2008.
15. Saxena, M.; Stephens, M. A.; Pathak, H.; Rangarajan, A. Transcription factors that mediate epithelial-mesenchymal transition lead to multidrug resistance by upregulating ABC transporters. *Cell Death Dis.* 2:e179; 2011.
16. Vega, S.; Morales, A. V.; Ocana, O. H.; Valdes, F.; Fabregat, I.; Nieto, M. A. Snail blocks the cell cycle and confers resistance to cell death. *Genes Dev.* 18:1131–43; 2004.
17. Wu, Y.; Zhou, B. P. New insights of epithelial-mesenchymal transition in cancer metastasis. *Acta Biochim. Biophys. Sin (Shanghai).* 40:643–50; 2008.
18. Ren, J.; Chen, Y.; Song, H.; Chen, L.; Wang, R. Inhibition of ZEB1 reverses EMT and chemoresistance in docetaxel-resistant human lung adenocarcinoma cell line. *J. Cell Biochem.* 114:1395–403; 2013.
19. Reed, J. C.; Miyashita, T.; Takayama, S.; Wang, H. G.; Sato, T.; Krajewski, S.; Aime-Sempe, C.; Bodrug, S.; Kitada, S.; Hanada, M. BCL-2 family proteins: Regulators of cell death involved in the pathogenesis of cancer and resistance to therapy. *J. Cell Biochem.* 60:23–32; 1996.
20. Zhang, L.; Yu, J.; Park, B. H.; Kinzler, K. W.; Vogelstein, B. Role of BAX in the apoptotic response to anticancer agents. *Science* 290:989–92; 2000.
21. Calatozzolo, C.; Gelati, M.; Ciusani, E.; Sciacca, F. L.; Pollo, B.; Cajola, L.; Marras, C.; Silvani, A.; Vitellaro-Zuccarello, L.; Croci, D.; Boiardi, A.; Salmaggi, A. Expression of drug resistance proteins Pgp, MRP1, MRP3, MRP5 and GST-pi in human glioma. *J. Neurooncol.* 74:113–21; 2005.
22. He, L.; Yang, C. P.; Horwitz, S. B. Mutations in beta-tubulin map to domains involved in regulation of microtubule stability in epothilone-resistant cell lines. *Mol. Cancer Ther.* 1:3–10; 2001.
23. Mehta, R. S.; Bornstein, R.; Yu, I. R.; Parker, R. J.; McLaren, C. E.; Nguyen, K. P.; Li, K. T.; Fruehauf, J. P. Breast cancer survival and in vitro tumor response in the extreme drug resistance assay. *Breast Cancer Res. Treat.* 66:225–37; 2001.
24. Loizzi, V.; Chan, J. K.; Osann, K.; Cappuccini, F.; DiSaia, P. J.; Berman, M. L. Survival outcomes in patients with recurrent ovarian cancer who were treated with chemoresistance assay-guided chemotherapy. *Am. J. Obstet. Gynecol.* 189:1301–7; 2003.
25. Holloway, R. W.; Mehta, R. S.; Finkler, N. J.; Li, K. T.; McLaren, C. E.; Parker, R. J.; Fruehauf, J. P. Association between in vitro platinum resistance in the EDR assay and clinical outcomes for ovarian cancer patients. *Gynecol. Oncol.* 87:8–16; 2002.
26. D'Amato, T. A.; Landreneau, R. J.; McKenna, R. J.; Santos, R. S.; Parker, R. J. Prevalence of in vitro extreme chemotherapy resistance in resected non small-cell lung cancer. *Ann. Thorac. Surg.* 81:440–6, 446–7; 2006.
27. Kern, D. H.; Weisenthal, L. M. Highly specific prediction of antineoplastic drug resistance with an in vitro assay using suprapharmacologic drug exposures. *J. Natl. Cancer Inst.* 82:582–8; 1990.